Molecular Therapy
Original Article

Long-Term Structural Outcomes of Late-Stage *RPE65* Gene Therapy

Kristin L. Gardiner,[1] Artur V. Cideciyan,[2] Malgorzata Swider,[2] Valérie L. Dufour,[1] Alexander Sumaroka,[2] András M. Komáromy,[3] William W. Hauswirth,[4] Simone Iwabe,[1] Samuel G. Jacobson,[2] William A. Beltran,[1] and Gustavo D. Aguirre[1]

[1]Division of Experimental Retinal Therapies, Department of Clinical Sciences & Advanced Medicine, School of Veterinary Medicine, University of Pennsylvania, Philadelphia, PA 19104, USA; [2]Scheie Eye Institute, Department of Ophthalmology, University of Pennsylvania Perelman School of Medicine, Philadelphia, PA 19104, USA; [3]Department of Small Animal Clinical Sciences, College of Veterinary Medicine, Michigan State University, East Lansing, MI 48824, USA; [4]Department of Ophthalmology, University of Florida, Gainesville, FL 32610, USA

The form of hereditary childhood blindness Leber congenital amaurosis (LCA) caused by biallelic RPE65 mutations is considered treatable with a gene therapy product approved in the US and Europe. The resulting vision improvement is well accepted, but long-term outcomes on the natural history of retinal degeneration are controversial. We treated four RPE65-mutant dogs in mid-life (age = 5–6 years) and followed them long-term (4–5 years). At the time of the intervention at mid-life, there were intra-ocular and inter-animal differences in local photoreceptor layer health ranging from near normal to complete degeneration. Treated locations having more than 63% of normal photoreceptors showed robust treatment-related retention of photoreceptors in the long term. Treated regions with less retained photoreceptors at the time of the intervention showed progressive degeneration similar to untreated regions with matched initial stage of disease. Unexpectedly, both treated and untreated regions in study eyes tended to show less degeneration compared to matched locations in untreated control eyes. These results support the hypothesis that successful long-term arrest of progression with RPE65 gene therapy may only occur in retinal regions with relatively retained photoreceptors at the time of the intervention, and there may be heretofore unknown mechanisms causing long-distance partial treatment effects beyond the region of subretinal injection.

INTRODUCTION

Building on two decades of previous research,[1–11] *RPE65* gene therapy was recently approved for marketing (Luxturna, voretigene neparvovec-rzyl) to provide improved functional vision to patients with biallelic *RPE65* mutations.[12,13] There is consensus that the therapy results in improvement of light sensitivity in the short term, and this is true in humans as well as mice and dogs.[14] Long-term consequences of the therapy on visual function and arrest of retinal degeneration, on the other hand, have been more controversial. Data from some investigators are consistent with the hypothesis that the natural rate of photoreceptor loss due to *RPE65* mutations is not modified by the gene therapy when treatments are initiated after the onset of degeneration,[9] and the short-term improvements in visual function start waning in the long term.[10,11] Data from others suggest that improved visual function is stable over the long term,[15] and they imply that retinal degeneration has been stabilized even though supporting photoreceptor layer measures have not been provided.

The molecular, biochemical, and cellular bases of the canine and human diseases are identical,[4,16,17] but the two have been treated at different disease stages. The initial work in *RPE65* mutant dogs, later validated by independent groups, treated young dogs in the early stages of the disease, when photoreceptor dysfunction and severe visual impairment were predominant but there was little degeneration.[2,4,9,18–20] The treatments showed rapid improvement in retinal, subcortical, and cortical visual function,[21] which remained stable long term.[9] Detailed analysis of retinal photoreceptors demonstrated distinct preservation of photoreceptor layer measures and structure in the treatment area 4.8–10.9 years after the initial treatment.[9]

However, treatment of dogs at mid-life gave more variable results.[9] While there was improvement of retinal function in all eyes initially, degeneration was not halted in some. Other eyes treated at mid-life had little evidence of retinal degeneration and required longer follow-up to allow quantitative evaluation of potential differences between treated and untreated regions.[9] In the present study, we have taken advantage of long-term (>4 years) observations and recognition of intra- and inter-retinal and inter-animal differences in the extent of retinal degeneration among treated mature dogs to determine the long-term outcomes of gene therapy initiated at mid-life.

Received 6 March 2019; accepted 14 August 2019;
https://doi.org/10.1016/j.ymthe.2019.08.013.

Correspondence: Gustavo D. Aguirre, Division of Experimental Retinal Therapies, Department of Clinical Sciences & Advanced Medicine, School of Veterinary Medicine, University of Pennsylvania, Philadelphia, PA 19104, USA.
E-mail: gda@vet.upenn.edu
Correspondence: Artur V. Cideciyan, Scheie Eye Institute, Department of Ophthalmology, University of Pennsylvania Perelman School of Medicine, Philadelphia, PA 19104, USA.
E-mail: cideciya@pennmedicine.upenn.edu

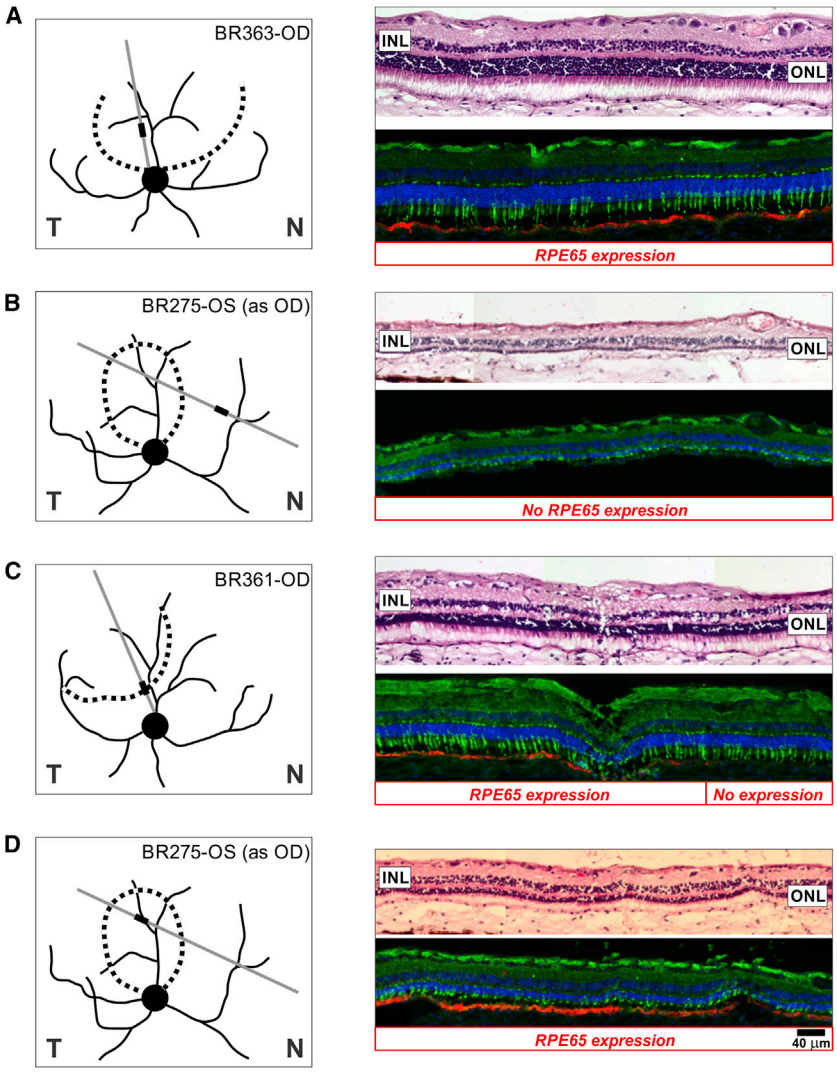

Figure 1. Gene Therapy and Photoreceptor Preservation

Subretinal gene therapy was performed in *RPE65* mutant dogs at mid-life (5–6 years), and eyes were collected 4–5 years later at 9–11 years of age for morphologic evaluation. Schematics show the treatment boundary (dotted lines) and illustrated area (thick lines) in the examined section (gray lines). Compared to the outcomes of treatments performed in young animals, there were both expected (A and B) and unexpected (C and D) features with mid-life treatment. Some retinal regions within the treated area showed RPE65 expression and retained photoreceptors (A), and some retinal regions outside the treated area showed no RPE65 expression and severe degeneration (B). However, some treatment boundaries had photoreceptor preservation continuing beyond the transduction region (C), and some treated regions showed substantial photoreceptor degeneration even with robust RPE65 expression (D). Section pairs stained with H&E (top) or dual immunolabeled with hCAR (green) and RPE65 (red) are shown. Scale bar, 40 µm applies to all sections. T, temporal retina; N, nasal retina. Labels such as BR363-OD refer to the animal and eye.

RESULTS

When retinas of 9- to 11-year-old *RPE65* mutant dogs were evaluated with serial sectioning 4–5 years after a single subretinal gene therapy injection, the results were not always uniform, or consistent, with the findings expected from injections performed previously in young animals. In dogs treated at mid-life (5–6 years old), some sections showed well-preserved photoreceptor nuclei with inner and outer segments (IS and OS) in retinal regions with intense RPE65 expression in the retinal pigment epithelium (RPE) (Figure 1A). Regions outside the treatment area showed absent or remnants of photoreceptors in regions with no RPE65 expression (Figure 1B), supporting the preliminary conclusion that successful gene therapy must have arrested the progressive photoreceptor degeneration over these long-term studies.

However, careful examination showed that there were also unexpected findings challenging this preliminary conclusion. In some retinal regions, photoreceptors and their inner and OS could be retained in retinal areas with no RPE65 expression, either in transition zones (Figure 1C) or more distant sites, or they showed substantial degeneration even when there was robust and uniform RPE65 expression (Figure 1D). There appeared to be a striking difference from previous subretinal gene therapy treatments in young animals, which always resulted in a well-defined and circumscribed area of photoreceptor preservation limited to the area of RPE65 expression when evaluated 7–10 years after treatment (e.g., see Figure 4 in Cideciyan et al.[9]). We hypothesized that the differences in local disease stage at the time of the treatment at mid-life and variability of progression rates across and between retinas may have contributed to the unexpected and variable findings.

Natural history of photoreceptor degeneration in *RPE65* mutant dogs can be approximated from previous work. Generally, mutant dogs younger than 4 years tend to retain near normal photoreceptors, whereas dogs older than 7 years tend to have severe retina-wide degeneration.[4,9,22] Available data are consistent with the onset of retinal degeneration occurring in the inferior and superior retinal regions variably between 4 and 7 years and progressing thereafter.[9] Photoreceptors along the visual streak region generally are retained the longest,[9] and this finding is not unlike human patients with retained central retinal regions.[23] This broad-brush view, however, does not capture the micro-topographical details of a variety of disease stages that may exist in neighboring regions intra-retinally, as well as inter-retinal differences at the time of treatment.

To gain insights into the variation of photoreceptor disease staging in canine mid-life and serve as a possible predictor of treatment outcomes, we mapped the outer nuclear layer (ONL) thickness topography of 13 *RPE65* mutant eyes and compared them to younger animals ~1 year of age and older animals 9–11 years of age (Figure 2). At 1 year, most *RPE65* mutant dogs had ONL thickness topography that was indistinguishable from wild-type (WT) control eyes (Figures 2A and 2B). By 9 years of age, there was severe retina-wide degeneration, with some eyes retaining a faint band of photoreceptors along the visual streak (Figure 2C). At mid-life (5–6 years), the ONL thickness distribution tended to be unpredictable with greater inter-animal variability (Figure 2D). Some of the eyes with the mildest stages of disease, as exemplified by BR304 at age 5.2 years, showed excellent photoreceptor and ONL preservation in the fovea-like region and the visual streak, as well as in regions inferior to the optic disc. In contrast, BR363 at the same age showed overall ONL thinning, especially in the visual streak and fovea-like region. However, the disease severity in these 2 dogs was still much less than in 2 other dogs, both 5.1 years of age, which displayed a dramatic loss of ONL as shown in the topographic maps (Figure 2D, BR323 and BR318). Even in the better preserved areas of BR318, thinning of the ONL was associated with shortened photoreceptor IS and a disordered OS layer (Figure 2D). At this more advanced stage of disease, the inter-animal differences were notable. Differences in disease stage in mid-life not only occurred between animals but also were observed intraocularly. It was clear that, within eyes, there were remarkable differences in disease severity, with inferior regions degenerating earlier and faster and patchy areas of preservation or degeneration occurring in a non-uniform distribution (Figure 2D).

The existence of the large differences in the distribution and stage of disease in mid-life across *RPE65* mutant dog retinas could potentially explain the variable long-term gene therapy outcomes. To better understand the microscopic correlates of in-life ONL topography measures, serial sections of retinal tissue blocks were taken that extended through the bleb and surrounding regions of treated eyes, and corresponding areas of the untreated fellow eyes. Although it was possible to get a reasonable approximation of the structural correlates from the tissue-trimming diagrams, it was essential to use features visible in both modalities in order to co-register histological results (such as RPE65 expression) with high spatial precision to in-life ONL thickness maps. Features detectable in both modalities included the optic nerve head boundaries, major blood vessel branchpoints, local retinal changes at the retinotomy site, localized band of retained ONL at the visual streak, and correlated changes of ONL thinning apparent on imaging at the fovea-like region at the center of the *area centralis* and the ganglion cell layer thickening apparent on histology.[24]

Results from the untreated eye of BR275 exemplify this approach and show the correspondence of the histologic and in-life assessments (Figure 3). For each eye, dozens of histological profiles of rows of ONL nuclei were quantified from histological serial sections (Figure 3A) and matched to ONL thickness profiles derived from in-life imaging (Figure 3B). Quantitative comparisons of the co-registered multimodality data from 2,079 sampled points across four untreated and four treated eyes suggested a linear relationship between ONL thickness measured on optical coherence tomography (OCT) and rows of ONL measured on histology, with a slope corresponding to 4.5 μm per row of nuclei (Figure 3C). These data were used to estimate retrospectively the histologic integrity of retina at the time of the treatment.

To determine the treatment effects of *RPE65* gene therapy, we first analyzed the histology from corresponding loci in treated study and uninjected fellow control eyes (Figure 4). At the age of histology, all dogs showed electroretinogram (ERG) asymmetry, demonstrating greater function summed across the treated retinas as compared to contralateral eyes (Figure S1), but the localized results were much more complex. Co-registered maps were used to select two areas along the visual streak, one inside and one outside the treatment bleb (Figures 4A–4D, schematics). Serial sections were stained with H&E, to assess photoreceptor and overall retinal structure, and dual immunolabeled with human cone arrestin (hCAR)/RPE65 or rod opsin/RPE65, to assess the two photoreceptor classes. All selected areas of study eyes showed evidence of progressive degeneration during the long-term experiments. Specifically, ONL layer thicknesses at the selected locations had thinned from 8.8 (±1.5) rows of nuclei (predicted from in-life imaging) at the time of the treatment to 6.5 (±1.6) rows of nuclei 4–5 years later (Figure 4). There was no apparent correlation between the extent of photoreceptor preservation and the existence of RPE65 expression. Areas that were better preserved, regardless of RPE65 expression, showed distinct labeling of cones with hCAR and rod OS with rod opsin (e.g., Figure 4A, study eyes). In some well-preserved areas outside the treatment region (e.g., Figure 4B, study eyes), the number of hCAR-labeled cones was decreased, but we could not determine if the loss was in the S- or L/M cone population as cone class-specific antibodies were not used. In areas with more advanced degeneration, hCAR-labeled cone IS were shortened or absent, and rod opsin-labeled OS were disorganized or absent (e.g., see Figures 4A and 4B, control eyes).

Unexpectedly, we found that untreated areas in the study eyes showed better photoreceptor preservation than corresponding locations in the fellow uninjected control eyes (Figure 4). For example, the untreated nasal visual streak region of BR275 was much better preserved with 6–7 rows of ONL nuclei than the comparable locus in the control eye with 4 rows of ONL nuclei. Similarly, the photoreceptor IS were elongated rather than shortened, and rod OS were organized rather than fragmented (Figure 4A, lower row). Untreated loci in the remaining three study eyes showed thicker ONL and better photoreceptor preservation as compared to matched locations in uninjected control eyes. The IS and OS were longer and normal or less fragmented; matched locations in the control eyes showed OS that were absent or fragmented and IS that were shortened or absent (Figures 4B–4D, lower rows).

The retinal topographic changes illustrated above for the visual streak region were extended across wider retinal regions by examining serial sections through treated and untreated areas of study eyes and

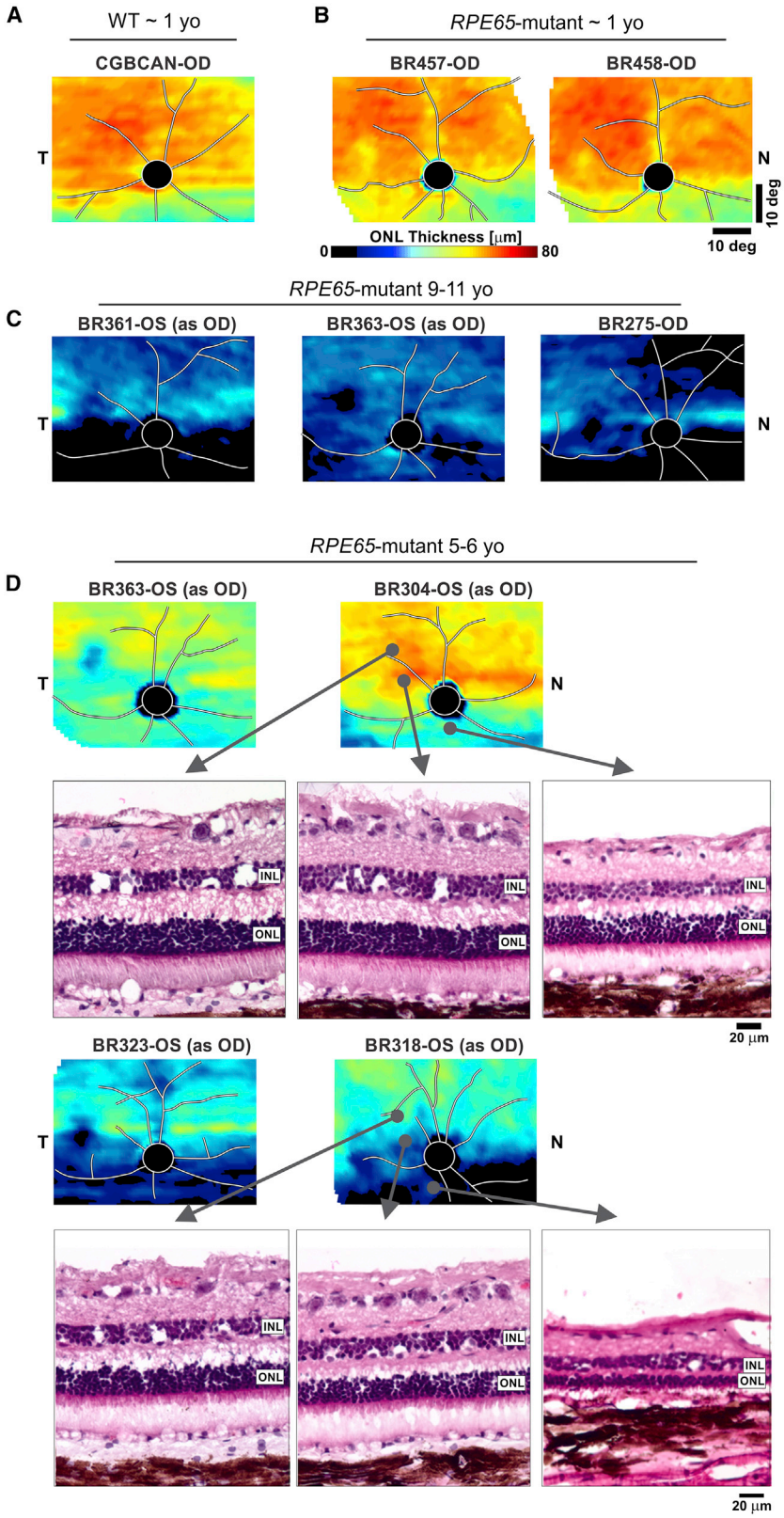

Figure 2. Natural History of Disease in *RPE65* Mutant Dogs Shows Great Variability

ONL thickness topographies (pseudocolor images) show representative 1-year-old *RPE65* mutant dogs (B) to have retained photoreceptors similar to normal wild-type (WT) dogs (A). In older dogs, 9–11 years of age, severe degeneration is common (C), but inter-animal and intra-retinal variability persists with selective but variable preservation of the horizontal visual streak. (D) At mid-life, between 5 and 6 years of age, mutant dogs show substantial variability such that retinal regions can range from normal to severely degenerated, and the variability can be intra-retinal. Histologic images are shown for three locations in two of the eyes.

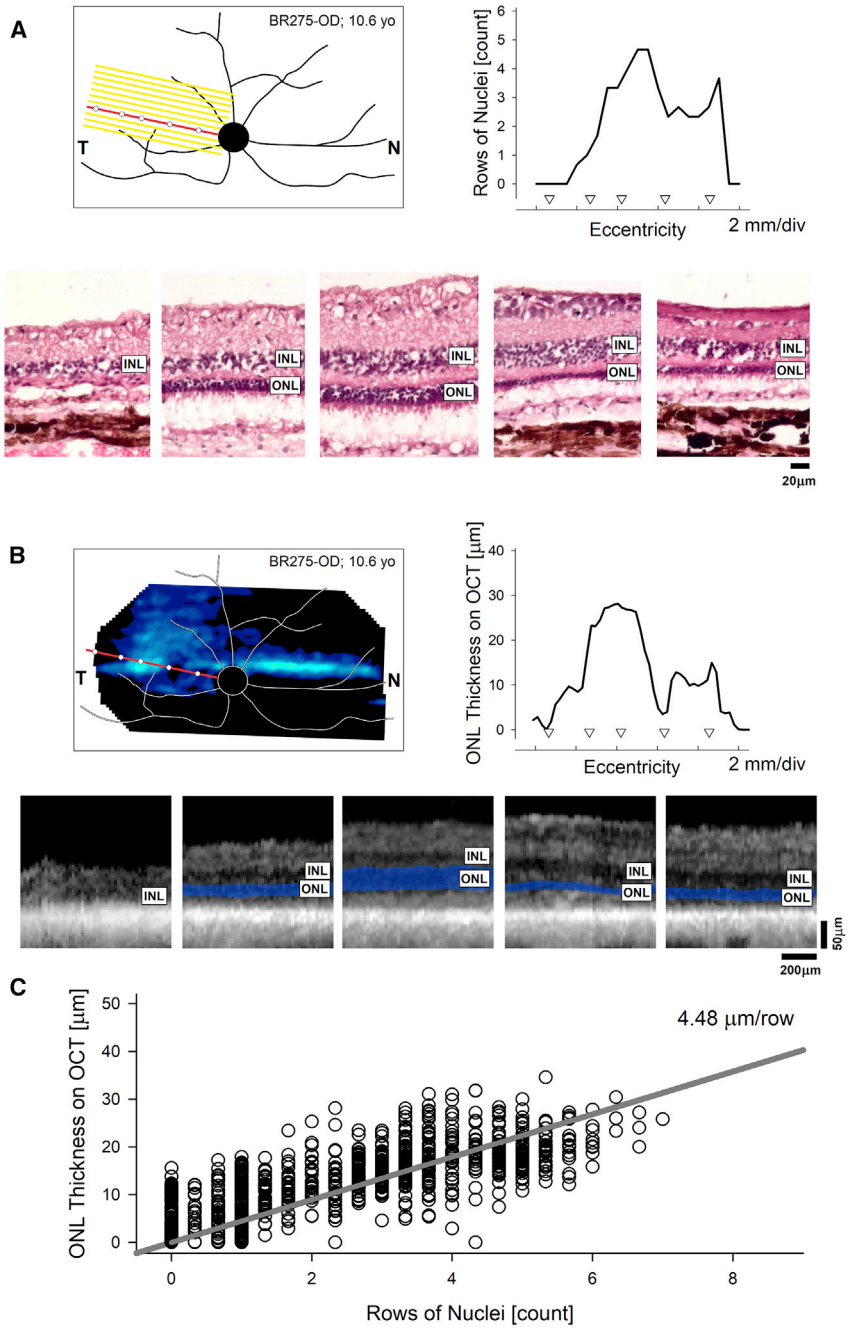

Figure 3. Histological Correlates of In-Life Imaging Results in *RPE65* Mutant Eyes

(A and B) Schematic representation of the retinal features of a representative eye overlaid with the localization of a block of serial sections (A, yellow parallel lines) or ONL thickness topography (B, pseudocolor image). The red oblique line represents the histologic section shown (A) or an optical coherence tomography (OCT) scan (B) registered to assess the same retinal region. The white circles superimposed on the red line are the corresponding points shown histologically (A, lower row) or in the OCT scan (B, lower row). The graphs in (A) and (B) represent the rows of nuclei counted on histologic sections (A) or the ONL thickness determined by OCT (B). INL, inner nuclear layer; ONL, outer nuclear layer. (C) Point-by-point correlation between ONL thickness and rows of nuclei determined from 2,079 co-registered loci across 8 mutant eyes at 9.4–10.6 years of age (Table S1).

equivalent areas in control eyes. This is illustrated with three of more than 400 serial sections taken from the treated eye of BR275-OS, for which we plotted ONL thickness, photoreceptor structure in terms of IS and OS structural preservation, and RPE65 expression (Figure 5). The most superior section (Figure 5A, B-B) showed robust RPE65 expression limited to the treatment area where photoreceptor preservation and ONL thickness were preserved (Figure 5B). Nasal to this area, photoreceptor preservation declined focally at the retinotomy site to then increase nasally as the section approached the nasal border of the visual streak. Even though there was no detectable RPE65 expression, and the site was at least 6 mm away from the injection bleb boundary, photoreceptor preservation and ONL thickness were comparable to the treatment area. Similar ONL thickness and photoreceptor preservation were observed in the bleb region in sections through the center (Figure 5A, C-C) and the lower parts of the treatment region (Figure 5A, D-D). Section C-C showed the drop-off temporally as the section extended supero-temporal from the treatment area and away from the temporal visual streak. However, the nasal region in this section showed recovery of photoreceptor structure and ONL thickness in the nasal visual streak area, which had no RPE65 expression (Figure 5C). This was not found in slide D-D, as the nasal extent was below the nasal visual streak and in an area of advanced degeneration (Figure 5D). Thus, assessment of therapy outcome was strongly dependent not only on expression of RPE65 but also on topography of treatment area in relation to sites that are preferentially preserved regardless of treatment.

We then asked if there was a requisite number of photoreceptors remaining at mid-life that could support long-term arrest of retinal degeneration with *RPE65* gene therapy. Because of the inter-animal and intra-retinal variation in disease severity, we addressed this question by determining the ONL topographic thickness in the study and control eyes for multiple specific retinal areas immediately before gene therapy. The loci selected were distributed within the (eventual) bleb area and the untreated non-bleb areas based on study eyes. The selection of loci was exactly duplicated in the uninjected control eyes. ONL thickness was obtained before treatment and at the end of study, 4–5 years later,

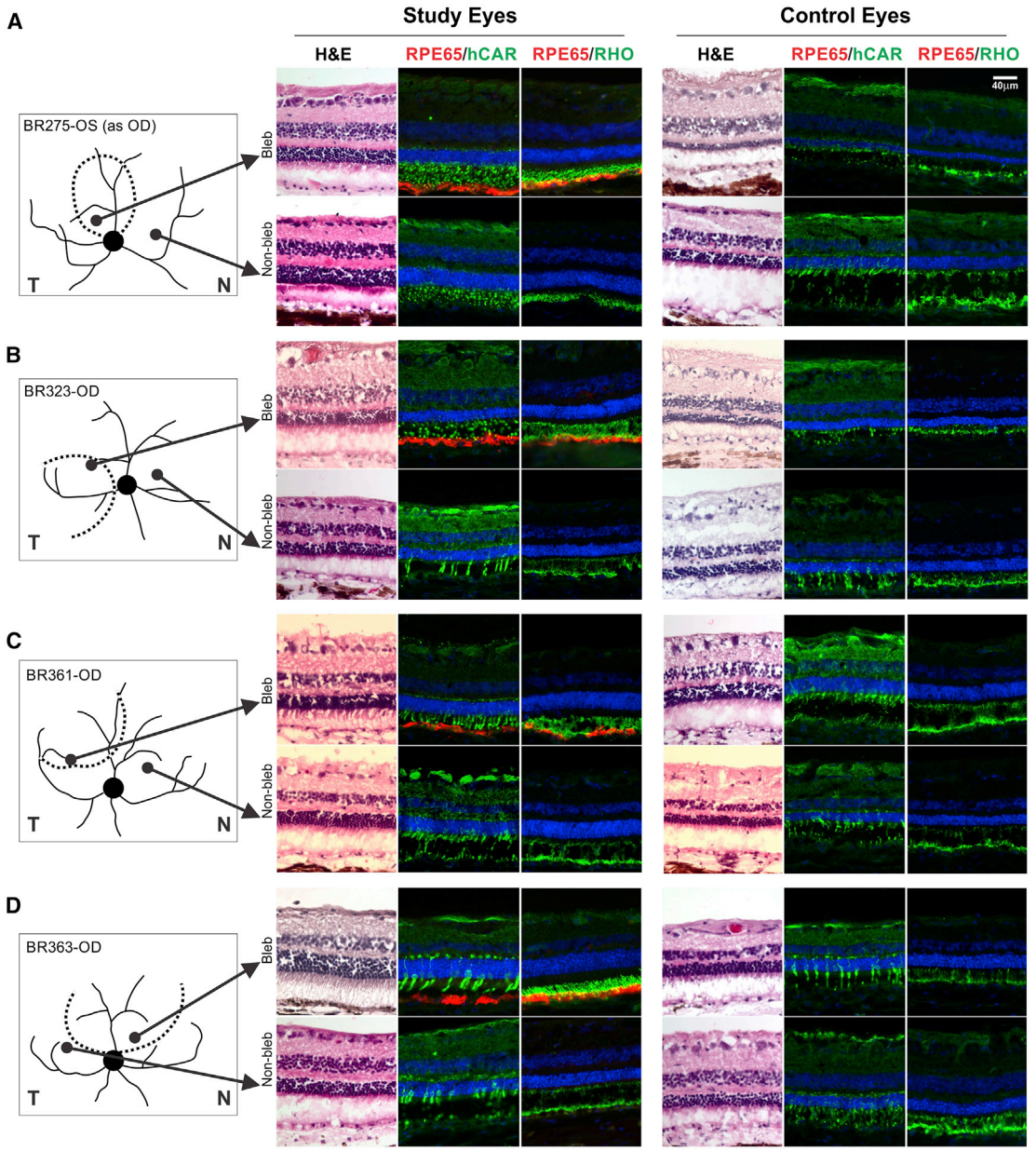

Figure 4. Histopathology from Matched Treated and Untreated Regions in Study and Uninjected Control Eyes

(A–D) Images represent sequential serial sections taken from inside (Bleb) or outside (Non-bleb) the treatment region. All samples are from the temporal or nasal visual streak, and the corresponding locations are illustrated for study and control eyes. Each image grouping shows H&E-stained sections (left) and immunocytochemistry sections dual labeled with RPE65 and hCAR (middle) or RPE65 and rod opsin (right); DAPI labels nuclei blue. RPE65 labeling is only present inside the treatment bleb. hCAR labels intensely the cone inner segments and synaptic terminals, and rod opsin the rod outer segments, and, when rod opsin is delocalized, the rod inner segments. Scale bar, 40 μm applies to all sections.

and progression was related to the ONL thickness at the time of treatment (Figure 6). A successful treatment effect of gene therapy was readily demonstrable for those bleb areas in study eyes where the ONL thickness at the time of treatment was within −0.2 log (63%) of WT values; progression observed long term was smaller than the progression in non-bleb areas with similarly mild disease (Figure 5B, left panel). Progression was −0.07 ± 0.05 log in the bleb region and −0.20 ± 0.10 log in the non-bleb region; the difference was statistically significant ($p = 2E{-}13$). When there was more advanced disease at the time of treatment, progression of ONL loss in bleb regions of study eyes was more marked (Figure 5B, right panel green symbols; −0.19 ± 0.21 log) and not substantially different from the progression

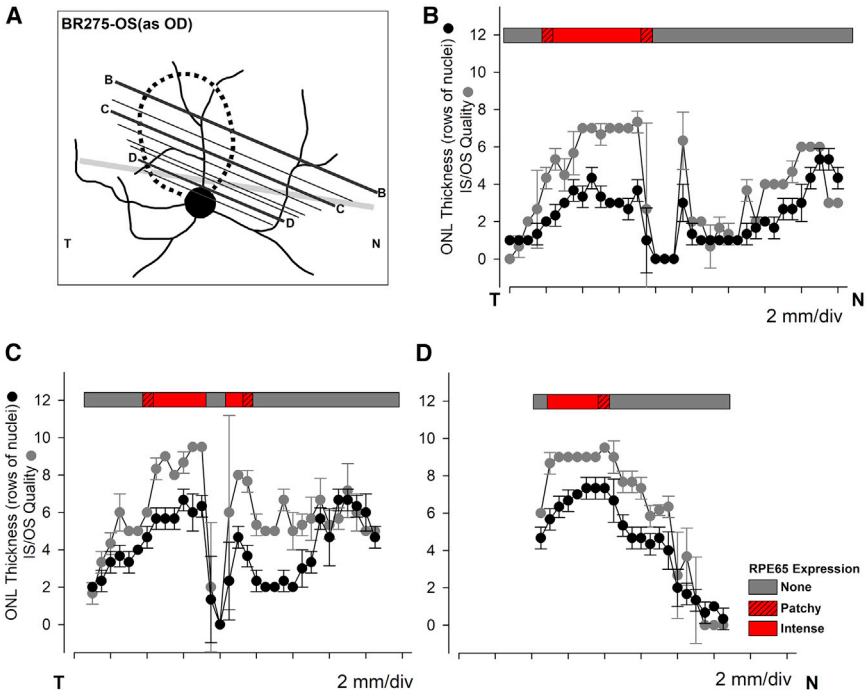

Figure 5. Association of RPE65 Expression with Preservation of Photoreceptors and ONL

(A) Schematic illustration of the treatment area (dotted line), and the location of a subset of more than 400 serial sections of which 40 were stained with H&E and analyzed for outer nuclear layer (ONL; rows of nuclei) thickness and photoreceptor preservation (inner and outer segments assessed separately and graded from 5 [normal] to 0 [absent] and values added). Each point in the graphs represents the mean ± SD for ONL (black filled circles) and photoreceptor structure (dark gray filled circles). RPE65 labeling determined from adjacent serial sections dual labeled with RPE65 and hCAR or RPE65 and rod opsin. The 3 sections illustrated in the graphs are 400 (B-B; B), 241 (C-C; C), and 63 (D-D; D). The thick gray line in (A) represents the expected location of the visual streak.

seen in non-bleb regions (Figure 5B, right panel red symbols; −0.27 ± 0.18 log; p = 0.06).

Uninjected control eyes showed a significantly faster rate of progression than study eyes irrespective of matched initial ONL thickness values both in bleb-equivalent (−0.41 ± 0.17 log) and non-bleb-equivalent (−0.44 ± 0.23 log) regions (Figures 5C and 5D, note expanded vertical scale). These quantitative in-life imaging results were consistent with the histological results described above, and they supported the proposal that a partial treatment effect may be extending to retinal areas well beyond the bleb formed by the subretinal injection, despite showing no evidence of RPE65 expression. These results taken together supported the conclusion that more than 63% of photoreceptors were required to be present at the time of the treatment to achieve *arrest* of retinal degeneration long term. For retinal locations with <63% of photoreceptors, evidence for a positive modification of the natural history depended on the control locations chosen; use of contralateral retina controls showed a treatment effect, whereas intra-retinal controls showed no treatment effect.

DISCUSSION

The successful treatment of the previously incurable *RPE65*-Leber congenital amaurosis (LCA) in animal models,[2,25] and the measured bench[19,26] to bedside[5–8] translation path[12] followed by the approval of the therapy for marketing in the United States and Europe has energized the research community, patient groups, and retinal specialists. Given the large number of inherited retinal disorders with complementary animal models,[27,28] the need is high, and the path from the laboratory to the clinic is accelerating rapidly. Gene therapy trials for diseases such as choroideremia, *CNGA3*- and *CNGB3*-achromatopsia, retinoschisis, and *RPGR*-X-linked retinitis pigmentosa among others also have been initiated (https://clinicaltrials.gov), and, based on exciting new results, studies for additional diseases, e.g., autosomal dominant rhodopsin (RHO) retinitis pigmentosa (RP)[29] and Best disease,[30] are in the IND-enabling pipeline.

The results of these very encouraging studies, however, must be tempered by having realistic, clear outcome measures, both short and long term, that inform on the therapeutic efficacy, limitations, and complications in both patients and animal models. After all, the goal of gene therapy for inherited retinal diseases is not only to improve vision but also to do so as permanently as possible and preferably with a single treatment. Hence, the important question, is the treatment forever? If not, then the studies need to have sufficient rigor to inform on what needs to be changed or improved to make it so.[31] However, clinical trial results in *RPE65*-LCA have erred toward simplification. The long wait for any therapy that can improve vision for inherited retinal degenerations has made affected patients and their families as well as clinical trialists and science writers[32] unreceptive to complexities and caveats about this remarkable achievement. Moreover, there have been no attempts to confirm or disprove findings by independently replicating such observations. There seems to be an attitude that the feat should be lauded and not critically evaluated; and effort should now be devoted to making this product available to those who could benefit from it ("…cannot allow the perfect to become the enemy of the good…"[33]). The route to marketing, the cost, and potential profits of the *RPE65*-LCA product have become models for other biotechnology and pharmaceutical companies in considering whether or how to become involved in treating orphan retinal diseases.

To address the long-term efficacy of *RPE65* gene therapy, we now have examined the treatment outcomes in the *RPE65*-LCA canine model

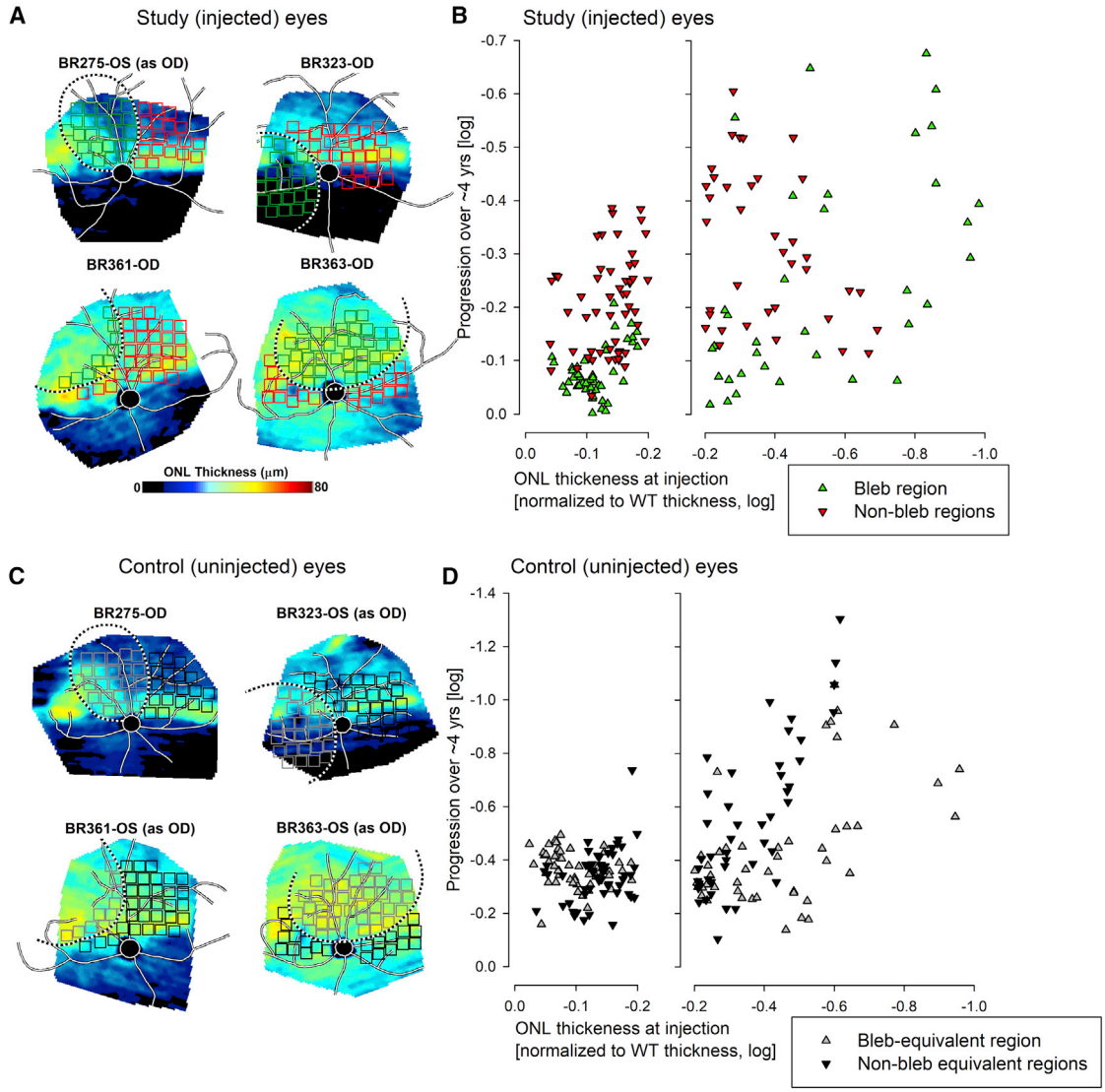

Figure 6. Progression of Photoreceptor Loss with Gene Therapy

(A and C) ONL thickness topography of study (A) and uninjected control (C) eyes to demonstrate the spatial variation of the retained photoreceptors at the time of treatment. Black and white dashed lines delineate the bleb region treated in study eyes (A) and the bleb-equivalent region in untreated controls (C). The small squares superimposed on the ONL thickness topographies indicate the locations sampled for ONL thickness (green/gray squares inside and red/black squares outside treatment bleb). (B and D) Change in ONL thickness over 4–5 years plotted against ONL thickness at the time of the treatment. ONL thickness values represent normalization to mean wild-type (WT) value at each sampled location and are shown in $\log_{10}$ units. Better preserved ONL regions (B, left panel) in treated areas of study eyes show limited to no progression (green symbols), while untreated regions show progression (red symbols). More severely affected areas (B, right panel) generally show progression regardless of treatment. Control eyes (D) with well preserved ONL in the bleb-equivalent region at the time of treatment (D, left panel) show comparable progression to the non-bleb-equivalent region. More severely affected areas (D, right panel) show greater progression. Note different scales for the ordinates of (B) and (D) to accommodate the greater progression seen in control eyes.

when the intervention is delayed to patient-relevant disease stages; i.e., when profound dysfunction is accompanied by varying degrees of photoreceptor degeneration. Our earlier studies indicated that when treatment is started at the stage of severe dysfunction, but before the onset of photoreceptor degeneration, the natural disease history is positively modified such that substantial numbers of photoreceptors are retained for up to a decade of follow-up along with preservation of retinal ERG function.[4,9] Similar but much shorter term outcomes have been reported by other groups;[20,34] as well, a morphologic/IHC study clearly showed that *RPE65* gene therapy slows the photoreceptor loss, especially of S-cones.[35]

The situation is more complex in a clinical setting where patients at the time of treatment have both severe visual dysfunction and

photoreceptor degeneration that is not uniformly distributed throughout the retina.[23,36–39] To model the characteristics of the patient's retinal disease, we selected for study the *RPE65* dog model at mid-life. Not surprisingly, there was considerable complexity in retinal disease patterns at this stage of life, when dysfunction and degeneration coexist and complicate the assessment of treatment outcomes. Issues to be considered include variations in disease severity, both within the treatment group at the same age and within the same eye. As well, the influence of topography on disease progression must be considered in that it might influence selective preservation in the absence of RPE65 transgene expression or, conversely, facilitate advancing degeneration in spite of robust expression.

Treatment outcomes in mid-life mutant dogs cannot be assessed strictly on an age basis, a caution that could equally apply to patient studies where some investigators have found age-related effects[40] whereas others have found none.[41] ONL thickness topography maps of dogs at 5–6 years of age show a marked difference in disease severity, ranging from nearly normal to advanced degeneration that is not uniformly distributed; as previously shown, the inferior retina degenerates earlier and faster.[9] However, the superior retina also degenerates, with some areas progressing faster (see Figure 2D). At this age as well as later, ONL thickness maps show a selective preservation of the visual streak, the elongated horizontal region located above the optic disc that tapers nasally and broadens temporally. This region has the highest density of retinal ganglion cells and cones, and it can be thought of as the canine equivalent to the primate macula. The broader temporal expanse of the visual streak is the *area centralis* in the center of which is the cone-enriched fovea-like region.[24] While the visual streak and *area centralis* are selectively preserved, the fovea-like region is not, and it clearly shows thinning/atrophy both in the ~5-year-old group and later at ~9–11 years (see Figures 2 and 3A). The focal atrophy of the fovea-like region has been previously described in *RPE65* mutant dogs,[42] and degeneration of this region is stabilized by gene therapy targeting the temporal quadrant.[35,43]

Because of the inter-animal and intra-retinal disease variability, it was necessary to precisely correlate *in vivo* and *ex vivo* analyses. The former is essential to determine the photoreceptor status at the time of treatment, and both to assess outcomes. Using landmarks visible in the *en face* images and serial histologic sections, it was possible to precisely register the OCT scans and histologic sections to obtain a good correlation of every point localized in the serial sections that is represented in ONL thickness maps. By comparing these loci, both inside/outside the treatment bleb with the same region in untreated fellow eyes, it was possible to determine the effect of disease stage and retinal topography on the treatment outcome.

We showed that areas where the ONL thickness was within 63% or greater of the WT controls at the time of treatment there was minimal if any progression. Areas with ONL thickness less than 63% of control generally progressed. Other factors to consider in determining outcomes include the extent and intensity of RPE65 expression. As expected, in many areas we found good correlation between RPE65 expression and photoreceptor preservation. However, we also observed degenerate areas having intense and uniform RPE65 expression. The pre-treatment ONL thickness maps provided insights, in some cases, about the discordant observation in that these areas had established degeneration at the time of treatment (e.g., refer to BR275-OS in Figures 1D and 6A). In such a case, one could argue that treatment restored RPE65 expression but could not prevent further degeneration.

An overall comparison of treated and untreated fellow eyes showed that treatment had a positive modification of the natural disease history, and, in treated eyes, this included areas outside the treatment bleb (see Figures 4 and 6). This was an unexpected finding, as we assumed that treatment effect would have been more restricted as in gene augmentation therapies that exclusively target photoreceptor cells, e.g., *CNGB3*-achromatopsia[44] and *RPGR*-X-linked RP (XLRP).[45] With *RPE65* gene therapy, on the other hand, treatment restores the retinoid cycle that ultimately results in production of the 11-*cis-retinal* chromophore needed for a functioning visual pigment.[46] If the photoreceptor preservation is mediated by the availability of additional 11-*cis-retinal* to photoreceptors, possible alternative routes could include diffusion through the retina and across the vitreous to distant sites, or diffusion through the interphotoreceptor matrix (IPM) by interphotoreceptor retinoid-binding protein (IRBP), the carrier for 11-*cis*-retinal.[47] Support for the former comes from studies of intravitreally administered 9-*cis-retinal*-conjugated chitosan, which restores ERG function in *RPE65* mutant dogs.[48] For the latter, we have found in this study and others that IRBP is expressed throughout the IPM in mutants, regardless of the degree of degeneration, until all photoreceptors are lost (data not shown and Gropp et al.[49]). Other alternatives to be considered, although less likely, are release of trophic factors due to surgical manipulation[50] and transduction of distant sites by vector leaking out of the retinotomy site.

Two prior studies argue against gene therapy having a positive effect beyond the zone of RPE65 expression in the treatment area. The first is by our group and suggested, possibly incorrectly, that 11-*cis*-retinal did not "diffuse across the retina but (was) restricted to the region of the subretinal injection."[4] While that was true for more distant inferior quadrant regions for injections placed supero-centrally, there is clearly detectable 11-*cis*-retinal in supero-temporal and -nasal regions (see Figure 2 and Table S1 in Acland et al.[4]). The second clearly showed that S-cone immunolabeling is lost beyond the point where RPE65 expression ends at the treatment edge (see Figures 5a–5c in Mowat et al.[35]). However, the integrity of the retina in areas of S-cone loss is normal, a suggestion that while S-cones may need higher levels of 11-*cis*-retinal for survival, the rods, which make up the bulk of the ONL, do not. While the question remains unanswered, it is clear that in treated eyes there is a small but detectable positive effect outside of the treatment zone, and this needs to be accounted for in assessing therapeutic outcomes.

In addition to a treatment effect by *RPE65* augmentation, retinal topography plays an important role in determining both the severity

of disease and its progression. The visual streak and *area centralis*, excluding the fovea-like region, are areas in the retinal mosaic that are more protected from disease severity and progression. This is clearly evident on the *en face* ONL thickness maps, which also show much more severe disease inferiorly, and in the serial sections, illustrating that there is better preservation in the nasal visual streak, far from the treatment bleb (see Figures 5B and 5D). At this time, it is not possible to determine the factor(s) that influences the topographic distribution of disease.

These results raise the clinically relevant question, are we able to compare the present canine results with those of human *RPE65*-LCA? To do so, we should ask whether young patients have any detectable retinal degeneration. There is no doubt that there can be major loss of photoreceptors and visual function in the later decades of life of *RPE65*-LCA patients.[36,38] In the canine model, retinal areas with ONL thickness $\geq$63% than in WT controls at the time of treatment showed minimal if any progression, while areas with less ONL thickness generally progressed. Are younger patients free of photoreceptor loss and, therefore, of no concern for durability of efficacy if treatment is administered at young ages?[23] Our study of photoreceptor topography in a cohort of untreated children and adolescents with *RPE65*-LCA quantified ONL thickness across a wide central retina of these patients and answers this question.[23] There were inter-individual differences between young patients, but not a single patient had normal photoreceptor layer thickness. Except at the fovea (with ~60% ONL thickness retained), the average maps of ONL showed thickness <40% of control across most of the central retina, and <20% in inferior retinal areas (see Figure 3 in Jacobson et al.[23]). Extrapolating from the current study in dogs to humans leads to the expectation that gene therapy treatment will not halt the progressive retinal degeneration in most retinal locations of *RPE65*-LCA patients at all ages. Of further importance to consider for the interpretation of human clinical trial results was the retained improvements of the global retinal function measure ERG in the current canine study while demonstrating major local evidence of degeneration. It follows that the stability of global measures of function in patients[15] does not rule out progressive degeneration as previously demonstrated, with local measures of structure and function following successful gene therapy.[9,10]

MATERIALS AND METHODS

Animals

All dogs were bred and maintained at the University of Pennsylvania Retinal Disease Studies Facility (RDSF; Table S1), and they were housed under identical conditions (e.g., diet, medications, vaccinations, and ambient illumination with cyclic 12 h on-12 h off). All but 1 of the *RPE65* mutants were females used to produce affected progeny for other studies or colony continuation, and they were enrolled in long-term studies that did not affect their reproductive status. Matings of these females had produced puppies: BR275, 1 time and BR323 and BR363, 2 times each; additionally, control female X236 had puppies 2 times. The studies were carried out in strict accordance with the recommendations in the Guide for the Care and Use of Laboratory Animals of the NIH and the USDA's Animal Welfare Act and Animal Welfare Regulations, and they complied with the Association for Research in Vision and Ophthalmology (ARVO) Statement for the Use of Animals in Ophthalmic and Vision Research. The protocols were approved by the Institutional Animal Care and Use Committee of the University of Pennsylvania (803269 and 804956). All electroretinographic and noninvasive imaging procedures, as well as subretinal injections, were performed under general anesthesia, as previously described.[24,45,51] Ocular tissues were collected after euthanasia with an intravenous injection of euthanasia solution (Euthasol; Virbac), and all efforts were made to improve animal welfare and minimize discomfort.

Vector and Subretinal Injections

Clinical-grade good manufacturing practice (GMP) vector produced for the phase 1/2 clinical trials was used. The adeno-associated virus serotype 2 (AAV2) vector has the cytomegalovirus (CMV) enhancer-chicken beta-actin exon 1-intron 1-exon 2 and the human *RPE65* cDNA.[7,8,19] In a prior study, the human and canine transgenes gave comparable short- and long-term therapeutic efficacy.[4] In the treated animals that were part of the study, the vector concentration used was 3.96×10^{11} vector genomes/mL, and injection volumes were in the 160- to 200-μL range (Table S1). This dose was comparable to the ones used in the human clinical trial.[7,41]

Subretinal injections of vector were performed under general anesthesia with a subretinal cannula, as previously reported (see below); the injected volumes aimed to produce a bleb that covered ~20%–25% of the retinal surface. The location of the subretinal bleb was recorded immediately after each injection. Short-term post-therapy treatment is standard in our protocols and has been previously described.[44,45,52] All of the dogs treated by *RPE65* gene augmentation therapy had recovery of ERG rod and cone function to variable degrees in the treated eyes 6 weeks after treatment, and function was still present, although reduced in amplitude, at the end of study.

OCT Imaging and Analyses

En face and retinal cross-sectional imaging was performed with the dogs under general anesthesia (induction with intravenous [i.v.] propofol; maintenance with isofluorane). Overlapping *en face* images of reflectivity with near-infrared illumination (820 nm) were obtained (Spectralis HRA+OCT, Heidelberg, Germany) with 30° and 55° diameter lenses to delineate fundus features, such as optic nerve, retinal blood vessels, boundaries of injection blebs, retinotomy sites, and other local changes. Custom programs (MATLAB 7.5; MathWorks, Natick, MA) were used to digitally stitch individual photos into a retina-wide panorama. Spectral domain-OCT (SD-OCT) was performed with linear and raster scans (Spectralis HRA+OCT). Overlapping 30° × 20° raster scans were recorded covering large regions of the retina. Post-acquisition processing of OCT data was performed with custom programs (MATLAB 7.5). For retina-wide topographic analysis, integrated backscatter intensity of each raster scan was used to locate its precise location and orientation relative to retinal features visible on the retina-wide mosaic formed by near infrared

(NIR) reflectance images. Individual longitudinal reflectivity profiles (LRPs) forming all registered raster scans were allotted to regularly spaced bins (1° × 1°) in a rectangular coordinate system centered at the optic nerve; LRPs in each bin were aligned and averaged. Intraretinal peaks and boundaries corresponding to the ONL were segmented using both intensity and slope information of backscatter signal along each LRP. For all topographic results, locations of blood vessels, optic nerve head, and bleb boundaries were overlaid for reference.

Morphological Evaluation

Embedding and Sectioning

RPE65-mutant (n = 6) and normal (n = 3) dogs were included in this study. Globes were harvested at varying endpoints in the study from dogs immediately following euthanasia and fixed/processed in the following manner: 4% paraformaldehyde (PFA) for 3 h, 2% PFA for 24 h, 15% sucrose in PBS for 24 h, and 30% sucrose in PBS for 24 h. The posterior eyecups were isolated at the end of the 4% PFA fixation step, and tissues were trimmed at the end of the 2% PFA fixation step. Based on the diagrams made at the end of the subretinal injection procedure, the eyecups were trimmed into quadrants or hemispheres in order to obtain sections from treated and untreated regions with a special emphasis for including boundaries or transition zones between treated and untreated regions. The trimmed tissues were placed into plastic sectioning molds containing optimum cutting temperature embedding media (Thermo Fisher Scientific, Waltham, MA) and flash frozen in liquid nitrogen. Thereafter, the tissue blocks were kept at −80°C.

IHC

Retinal localization and expression of selected proteins, RPE65, hCAR, RHO, and IRBP, were performed by double-labeling IHC using methods previously described.[53,54] Slides were warmed to 37°C for 1 h, then incubated overnight at 4°C with the first primary antibody (anti-RPE65, mouse monoclonal immunoglobulin G (IgG)1, 1:1,000 dilution, Novus Biologicals, Littleton, CO, NB100-355, lot#K-1), then subsequently with fluorochrome-labeled secondary antibody (1:200 dilution of donkey anti-mouse IgG, Alexa Fluor 568, A10037, Invitrogen, Carlsbad, CA) at room temperature for 2 h. The samples were then incubated overnight with the second primary antibody (either rabbit polyclonal anti-RHO (1:1,000 dilution, Millipore Sigma, Burlington, MA, AB9279, lot#2979895), goat polyclonal anti-hCAR (1:50), or rabbit polyclonal anti-IRBP (1:1,000 dilution, gift from Dr. T.M. Redmond, National Eye Institute [NEI]/NIH), then labeled with the second secondary antibody (either 1:200 dilution of donkey anti-rabbit IgG, A21206, or 1:200 dilution of donkey anti-goat IgG, A11055, Alexa Fluor 488, Invitrogen), and cell nuclei stained with DAPI. The slides were mounted with Gelvatol (pH 8.5; Sigma-Aldrich, St. Louis, MO) and dried at room temperature overnight, then subsequently stored at 4°C. Labeled slides were examined with an epifluorescence microscope (Axioplan, Carl Zeiss Meditec, Thornwood, NY). Transmitted light and epifluorescence images were obtained with a Spot 4.0 camera (Diagnostic Instruments, Sterling Heights, MI) and examined with Photoshop and Illustrator (Adobe, San Jose, CA). For each antibody, control and affected canine samples were processed at the same time with the same antibody concentration and lot number; when capturing images for documentation, the same magnification and camera settings were used in all the samples.

Photoreceptor and RPE Evaluation

The tissue blocks were serial sectioned, and every tenth section was H&E stained. Using a standard Zeiss binocular microscope and both 20× and 40× objectives, each section (~8,500- to 14,000-μm total distance) was fully examined in 500-μm increments. At each point, ONL thickness was determined by making 3 independent counts of the number of rows of nuclei from the center and either side of the field of view. As well, photoreceptor structural integrity was assessed independently for OS and IS using the following criteria: OS, normal, disordered, fragmented, absent; IS, normal, shortened, absent, and represented graphically in Figure 5 spidergrams as the sum of OS and IS gradings from normal (5) to absent (0) for each. The slides immediately adjacent on either side of the H&E sections were dual labeled with a combination of RPE65/hCAR or RPE65/RHO to characterize RPE65 expression in the treated and untreated regions and to further determine quality of photoreceptor structure and preservation. RPE65 labeling was classified as intense, patchy, or absent.

Alignment of OCT Scans and Retinal Sections

To properly align the retinal sections with the *en face* images, the sections were oriented based on the trimming and embedding records, section number, optic nerve head position, retinotomy site, ONL thickness, and blood vessel branching landmarks. From the ONL thickness counts, a mean ONL thickness value was generated at each specific retinal locus and compared to ONL thickness from topographic maps for the length of each section. Retinal blood vessel position was also measured for each H&E section and compared with *en face* images. Using a combination of these objective measurements, the degrees of freedom could be limited such that the angle of the sections could be properly oriented and overlaid on the *en face* images. The OCT data generated at each time point could also be superimposed over the same *en face* retina images, which allowed for direct comparison of the OCT measurements at each retina location and the ONL thickness on histology.

Statistical Methods

Descriptive statistics including mean and SD were used. Group means were compared with unpaired t tests.

Electroretinography

Full-field flash ERGs were recorded under general anesthesia (induction with i.v. propofol; maintenance with isofluorane) using a custom-built Ganzfeld dome fitted with the light emitting diode (LED) stimuli of a ColorDome stimulator (Diagnosys) and methods previously described.[51] Waveforms were processed with a digital low-pass (50-Hz) filter to reduce recording noise if necessary. After 20 min of dark adaptation, rod and mixed rod-cone-mediated responses were recorded. Following 5 min of white light adaptation, cone-mediated

signals to a series of single flashes and to 29-Hz flicker stimuli were recorded.

SUPPLEMENTAL INFORMATION

Supplemental Information can be found online at https://doi.org/10.1016/j.ymthe.2019.08.013.

AUTHOR CONTRIBUTIONS

K.L.G. developed the methods for histologic analysis and carried out the experiments, validated the results, and reviewed and edited drafts and the final manuscript. A.V.C. and G.D.A. developed the research goals and methodology, carried out formal analysis, wrote original and final drafts, and supervised the research activity. M.S. developed methods for correlating *in vivo* and *ex vivo* data and presenting the results in figures used in the paper. V.L.D., A.M.K. and S.I. carried out different aspects of the *in vivo* studies. A.S. analyzed OCT data. W.W.H. provided vectors. S.G.J. and W.A.B. provided critical review and advice at different stages of the study and were involved in the review and editing of the original draft of the manuscript.

CONFLICTS OF INTEREST

G.D.A., W.W.H., and S.G.J. are patent holders for the RPE65 gene therapy patent filed jointly by the University of Pennsylvania on behalf of the University of Florida and Cornell University. In regards to this patent, S.G.J. has signed away all financial interests that may accrue. In addition, W.W.H. owns stock in the companies AGTC and BionicSight and is a paid consultant and on the scientific board of AGTC.

ACKNOWLEDGMENTS

The project was supported in part by grants R01 EY006855, EY017549, EY019304, and EY025752 from the National Eye Institute. The content is solely the responsibility of the authors and does not necessarily represent the official views of the National Eye Institute or the NIH. Additional support from the Foundation Fighting Blindness, the Van Sloun Fund for Canine Genetic Research, and the BrightFocus Foundation is acknowledged, as is the partial stipend support for K.L.G. provided by the office of the Vice Provost for Research at the University of Pennsylvania. The authors thank Drs. Luis Felipe Marinho and José M. Guzmán of the University of Pennsylvania for clinical examinations of the dogs in the early phases of the study, Vince Chiodo of the University of Florida for vector and vector construct details, Svetlana Savina and Evelyn Santana for technical support, Terry Jordan and the staff of RDSF for excellent animal care and support in all *in vivo* studies, and Lydia Melnyk for research coordination.

REFERENCES

1. Redmond, T.M., Yu, S., Lee, E., Bok, D., Hamasaki, D., Chen, N., Goletz, P., Ma, J.X., Crouch, R.K., and Pfeifer, K. (1998). Rpe65 is necessary for production of 11-cis-vitamin A in the retinal visual cycle. Nat. Genet. *20*, 344–351.

2. Acland, G.M., Aguirre, G.D., Ray, J., Zhang, Q., Aleman, T.S., Cideciyan, A.V., Pearce-Kelling, S.E., Anand, V., Zeng, Y., Maguire, A.M., et al. (2001). Gene therapy restores vision in a canine model of childhood blindness. Nat. Genet. *28*, 92–95.

3. Dejneka, N.S., Surace, E.M., Aleman, T.S., Cideciyan, A.V., Lyubarsky, A., Savchenko, A., Redmond, T.M., Tang, W., Wei, Z., Rex, T.S., et al. (2004). In utero gene therapy rescues vision in a murine model of congenital blindness. Mol. Ther. *9*, 182–188.

4. Acland, G.M., Aguirre, G.D., Bennett, J., Aleman, T.S., Cideciyan, A.V., Bennicelli, J., Dejneka, N.S., Pearce-Kelling, S.E., Maguire, A.M., Palczewski, K., et al. (2005). Long-term restoration of rod and cone vision by single dose rAAV-mediated gene transfer to the retina in a canine model of childhood blindness. Mol. Ther. *12*, 1072–1082.

5. Bainbridge, J.W., Smith, A.J., Barker, S.S., Robbie, S., Henderson, R., Balaggan, K., Viswanathan, A., Holder, G.E., Stockman, A., Tyler, N., et al. (2008). Effect of gene therapy on visual function in Leber's congenital amaurosis. N. Engl. J. Med. *358*, 2231–2239.

6. Maguire, A.M., Simonelli, F., Pierce, E.A., Pugh, E.N., Jr., Mingozzi, F., Bennicelli, J., Banfi, S., Marshall, K.A., Testa, F., Surace, E.M., et al. (2008). Safety and efficacy of gene transfer for Leber's congenital amaurosis. N. Engl. J. Med. *358*, 2240–2248.

7. Hauswirth, W.W., Aleman, T.S., Kaushal, S., Cideciyan, A.V., Schwartz, S.B., Wang, L., Conlon, T.J., Boye, S.L., Flotte, T.R., Byrne, B.J., and Jacobson, S.G. (2008). Treatment of leber congenital amaurosis due to RPE65 mutations by ocular subretinal injection of adeno-associated virus gene vector: short-term results of a phase I trial. Hum. Gene Ther. *19*, 979–990.

8. Cideciyan, A.V., Aleman, T.S., Boye, S.L., Schwartz, S.B., Kaushal, S., Roman, A.J., Pang, J.J., Sumaroka, A., Windsor, E.A., Wilson, J.M., et al. (2008). Human gene therapy for RPE65 isomerase deficiency activates the retinoid cycle of vision but with slow rod kinetics. Proc. Natl. Acad. Sci. USA *105*, 15112–15117.

9. Cideciyan, A.V., Jacobson, S.G., Beltran, W.A., Sumaroka, A., Swider, M., Iwabe, S., Roman, A.J., Olivares, M.B., Schwartz, S.B., Komáromy, A.M., et al. (2013). Human retinal gene therapy for Leber congenital amaurosis shows advancing retinal degeneration despite enduring visual improvement. Proc. Natl. Acad. Sci. USA *110*, E517–E525.

10. Jacobson, S.G., Cideciyan, A.V., Roman, A.J., Sumaroka, A., Schwartz, S.B., Heon, E., and Hauswirth, W.W. (2015). Improvement and decline in vision with gene therapy in childhood blindness. N. Engl. J. Med. *372*, 1920–1926.

11. Bainbridge, J.W., Mehat, M.S., Sundaram, V., Robbie, S.J., Barker, S.E., Ripamonti, C., Georgiadis, A., Mowat, F.M., Beattie, S.G., Gardner, P.J., et al. (2015). Long-term effect of gene therapy on Leber's congenital amaurosis. N. Engl. J. Med. *372*, 1887–1897.

12. Russell, S., Bennett, J., Wellman, J.A., Chung, D.C., Yu, Z.F., Tillman, A., Wittes, J., Pappas, J., Elci, O., McCague, S., et al. (2017). Efficacy and safety of voretigene neparvovec (AAV2-hRPE65v2) in patients with RPE65-mediated inherited retinal dystrophy: a randomised, controlled, open-label, phase 3 trial. Lancet *390*, 849–860.

13. Maguire, A.M., Russell, S., Wellman, J.A., Chung, D.C., Yu, Z.-F., Tillman, A., Wittes, J., Pappas, J., Elci, O., Marshall, K.A., et al. (2019). Efficacy, safety, and durability of voretigene neparvovec-rzyl in RPE65 mutation-associated inherited retinal dystrophy: Results of phase 1 and 3 trials. Ophthalmology *126*, 1273–1285.

14. Cideciyan, A.V. (2010). Leber congenital amaurosis due to RPE65 mutations and its treatment with gene therapy. Prog. Retin. Eye Res. *29*, 398–427.

15. Ashtari, M., Nikonova, E.S., Marshall, K.A., Young, G.J., Aravand, P., Pan, W., Ying, G.S., Willett, A.E., Mahmoudian, M., Maguire, A.M., and Bennett, J. (2017). The role of the human visual cortex in assessment of the long-term durability of retinal gene therapy in follow-on RPE65 clinical trial patients. Ophthalmology *124*, 873–883.

16. Gu, S.M., Thompson, D.A., Srikumari, C.R., Lorenz, B., Finckh, U., Nicoletti, A., Murthy, K.R., Rathmann, M., Kumaramanickavel, G., Denton, M.J., and Gal, A. (1997). Mutations in RPE65 cause autosomal recessive childhood-onset severe retinal dystrophy. Nat. Genet. *17*, 194–197.

17. Aguirre, G.D., Baldwin, V., Pearce-Kelling, S., Narfström, K., Ray, K., and Acland, G.M. (1998). Congenital stationary night blindness in the dog: common mutation in the RPE65 gene indicates founder effect. Mol. Vis. *4*, 23–29.

18. Narfström, K., Katz, M.L., Bragadottir, R., Seeliger, M., Boulanger, A., Redmond, T.M., Caro, L., Lai, C.M., and Rakoczy, P.E. (2003). Functional and structural recovery of the retina after gene therapy in the RPE65 null mutation dog. Invest. Ophthalmol. Vis. Sci. *44*, 1663–1672.

19. Jacobson, S.G., Acland, G.M., Aguirre, G.D., Aleman, T.S., Schwartz, S.B., Cideciyan, A.V., Zeiss, C.J., Komaromy, A.M., Kaushal, S., Roman, A.J., et al. (2006). Safety of recombinant adeno-associated virus type 2-RPE65 vector delivered by ocular subretinal injection. Mol. Ther. *13*, 1074–1084.

20. Le Meur, G., Stieger, K., Smith, A.J., Weber, M., Deschamps, J.Y., Nivard, D., Mendes-Madeira, A., Provost, N., Péréon, Y., Cherel, Y., et al. (2007). Restoration of vision in RPE65-deficient Briard dogs using an AAV serotype 4 vector that specifically targets the retinal pigmented epithelium. Gene Ther. *14*, 292–303.

21. Aguirre, G.K., Komáromy, A.M., Cideciyan, A.V., Brainard, D.H., Aleman, T.S., Roman, A.J., Avants, B.B., Gee, J.C., Korczykowski, M., Hauswirth, W.W., et al. (2007). Canine and human visual cortex intact and responsive despite early retinal blindness from RPE65 mutation. PLoS Med. *4*, e230.

22. Wrigstad, A., Narfstrom, K., and Nilsson, S.E. (1994). Slowly progressive changes of the retina and retinal pigment epithelium in Briard dogs with hereditary retinal dystrophy. A morphological study. Doc. Ophthalmol. *87*, 337–354.

23. Jacobson, S.G., Cideciyan, A.V., Aleman, T.S., Sumaroka, A., Windsor, E.A., Schwartz, S.B., Heon, E., and Stone, E.M. (2008). Photoreceptor layer topography in children with leber congenital amaurosis caused by RPE65 mutations. Invest. Ophthalmol. Vis. Sci. *49*, 4573–4577.

24. Beltran, W.A., Cideciyan, A.V., Guziewicz, K.E., Iwabe, S., Swider, M., Scott, E.M., Savina, S.V., Ruthel, G., Stefano, F., Zhang, L., et al. (2014). Canine retina has a primate fovea-like bouquet of cone photoreceptors which is affected by inherited macular degenerations. PLoS ONE *9*, e90390.

25. Chen, Y., Moiseyev, G., Takahashi, Y., and Ma, J.X. (2006). RPE65 gene delivery restores isomerohydrolase activity and prevents early cone loss in Rpe65-/- mice. Invest. Ophthalmol. Vis. Sci. *47*, 1177–1184.

26. Jacobson, S.G., Boye, S.L., Aleman, T.S., Conlon, T.J., Zeiss, C.J., Roman, A.J., Cideciyan, A.V., Schwartz, S.B., Komaromy, A.M., Doobrajh, M., et al. (2006). Safety in nonhuman primates of ocular AAV2-RPE65, a candidate treatment for blindness in Leber congenital amaurosis. Hum. Gene Ther. *17*, 845–858.

27. Baehr, W., and Frederick, J.M. (2009). Naturally occurring animal models with outer retina phenotypes. Vision Res. *49*, 2636–2652.

28. Petersen-Jones, S.M., and Komáromy, A.M. (2015). Dog models for blinding inherited retinal dystrophies. Hum. Gene Ther. Clin. Dev. *26*, 15–26.

29. Cideciyan, A.V., Sudharsan, R., Dufour, V.L., Massengill, M.T., Iwabe, S., Swider, M., Lisi, B., Sumaroka, A., Marinho, L.F., Appelbaum, T., et al. (2018). Mutation-independent rhodopsin gene therapy by knockdown and replacement with a single AAV vector. Proc. Natl. Acad. Sci. USA *115*, E8547–E8556.

30. Guziewicz, K.E., Cideciyan, A.V., Beltran, W.A., Komáromy, A.M., Dufour, V.L., Swider, M., Iwabe, S., Sumaroka, A., Kendrick, B.T., Ruthel, G., et al. (2018). *BEST1* gene therapy corrects a diffuse retina-wide microdetachment modulated by light exposure. Proc. Natl. Acad. Sci. USA *115*, E2839–E2848.

31. Jacobson, S.G., Cideciyan, A.V., Aguirre, G.D., Roman, A.J., Sumaroka, A., Hauswirth, W.W., and Palczewski, K. (2015). Improvement in vision: a new goal for treatment of hereditary retinal degenerations. Expert Opin. Orphan Drugs *3*, 563–575.

32. Lewis, R. (2012). The Forever Fix: Gene Therapy and the Boy Who Saved It (New York: St. Martin's Press).

33. Wojno, A.P., Pierce, E.A., and Bennett, J. (2013). Seeing the light. Sci. Transl. Med. *5*, 175fs8.

34. Bennicelli, J., Wright, J.F., Komaromy, A., Jacobs, J.B., Hauck, B., Zelenaia, O., Mingozzi, F., Hui, D., Chung, D., Rex, T.S., et al. (2008). Reversal of blindness in animal models of leber congenital amaurosis using optimized AAV2-mediated gene transfer. Mol. Ther. *16*, 458–465.

35. Mowat, F.M., Breuwer, A.R., Bartoe, J.T., Annear, M.J., Zhang, Z., Smith, A.J., Bainbridge, J.W., Petersen-Jones, S.M., and Ali, R.R. (2013). RPE65 gene therapy slows cone loss in Rpe65-deficient dogs. Gene Ther. *20*, 545–555.

36. Jacobson, S.G., Aleman, T.S., Cideciyan, A.V., Sumaroka, A., Schwartz, S.B., Windsor, E.A., Traboulsi, E.I., Heon, E., Pittler, S.J., Milam, A.H., et al. (2005). Identifying photoreceptors in blind eyes caused by RPE65 mutations: Prerequisite for human gene therapy success. Proc. Natl. Acad. Sci. USA *102*, 6177–6182.

37. Jacobson, S.G., Aleman, T.S., Cideciyan, A.V., Heon, E., Golczak, M., Beltran, W.A., Sumaroka, A., Schwartz, S.B., Roman, A.J., Windsor, E.A., et al. (2007). Human cone photoreceptor dependence on RPE65 isomerase. Proc. Natl. Acad. Sci. USA *104*, 15123–15128.

38. Jacobson, S.G., Aleman, T.S., Cideciyan, A.V., Roman, A.J., Sumaroka, A., Windsor, E.A., Schwartz, S.B., Heon, E., and Stone, E.M. (2009). Defining the residual vision in leber congenital amaurosis caused by RPE65 mutations. Invest. Ophthalmol. Vis. Sci. *50*, 2368–2375.

39. Caruso, R.C., Aleman, T.S., Cideciyan, A.V., Roman, A.J., Sumaroka, A., Mullins, C.L., Boye, S.L., Hauswirth, W.W., and Jacobson, S.G. (2010). Retinal disease in Rpe65-deficient mice: comparison to human leber congenital amaurosis due to RPE65 mutations. Invest. Ophthalmol. Vis. Sci. *51*, 5304–5313.

40. Maguire, A.M., High, K.A., Auricchio, A., Wright, J.F., Pierce, E.A., Testa, F., Mingozzi, F., Bennicelli, J.L., Ying, G.S., Rossi, S., et al. (2009). Age-dependent effects of RPE65 gene therapy for Leber's congenital amaurosis: a phase 1 dose-escalation trial. Lancet *374*, 1597–1605.

41. Jacobson, S.G., Cideciyan, A.V., Ratnakaram, R., Heon, E., Schwartz, S.B., Roman, A.J., Peden, M.C., Aleman, T.S., Boye, S.L., Sumaroka, A., et al. (2012). Gene therapy for leber congenital amaurosis caused by RPE65 mutations: safety and efficacy in 15 children and adults followed up to 3 years. Arch. Ophthalmol. *130*, 9–24.

42. Mowat, F.M., Gervais, K.J., Occelli, L.M., Annear, M.J., Querubin, J., Bainbridge, J.W., Smith, A.J., Ali, R.R., and Petersen-Jones, S.M. (2017). Early-onset progressive degeneration of the area centralis in RPE65-deficient dogs. Invest. Ophthalmol. Vis. Sci. *58*, 3268–3277.

43. Mowat, F.M., Petersen-Jones, S.M., Williamson, H., Williams, D.L., Luthert, P.J., Ali, R.R., and Bainbridge, J.W. (2008). Topographical characterization of cone photoreceptors and the area centralis of the canine retina. Mol. Vis. *14*, 2518–2527.

44. Komáromy, A.M., Alexander, J.J., Rowlan, J.S., Garcia, M.M., Chiodo, V.A., Kaya, A., Tanaka, J.C., Acland, G.M., Hauswirth, W.W., and Aguirre, G.D. (2010). Gene therapy rescues cone function in congenital achromatopsia. Hum. Mol. Genet. *19*, 2581–2593.

45. Beltran, W.A., Cideciyan, A.V., Lewin, A.S., Iwabe, S., Khanna, H., Sumaroka, A., Chiodo, V.A., Fajardo, D.S., Román, A.J., Deng, W.T., et al. (2012). Gene therapy rescues photoreceptor blindness in dogs and paves the way for treating human X-linked retinitis pigmentosa. Proc. Natl. Acad. Sci. USA *109*, 2132–2137.

46. Saari, J.C. (2000). Biochemistry of visual pigment regeneration: the Friedenwald lecture. Invest. Ophthalmol. Vis. Sci. *41*, 337–348.

47. Chader, G.J. (1989). Interphotoreceptor retinoid-binding protein (IRBP): a model protein for molecular biological and clinically relevant studies. Friedenwald lecture. Invest. Ophthalmol. Vis. Sci. *30*, 7–22.

48. Gao, S., Kahremany, S., Zhang, J., Jastrzebska, B., Querubin, J., Petersen-Jones, S.M., and Palczewski, K. (2018). Retinal-chitosan conjugates effectively deliver active chromophores to retinal photoreceptor cells in blind mice and dogs. Mol. Pharmacol. *93*, 438–452.

49. Gropp, K.E., Huang, J.C., and Aguirre, G.D. (1997). Differential expression of photoreceptor-specific proteins during disease and degeneration in the progressive rod-cone degeneration (prcd) retina. Exp. Eye Res. *64*, 875–886.

50. Faktorovich, E.G., Steinberg, R.H., Yasumura, D., Matthes, M.T., and LaVail, M.M. (1992). Basic fibroblast growth factor and local injury protect photoreceptors from light damage in the rat. J. Neurosci. *12*, 3554–3567.

51. Beltran, W.A., Cideciyan, A.V., Iwabe, S., Swider, M., Kosyk, M.S., McDaid, K., Martynyuk, I., Ying, G.S., Shaffer, J., Deng, W.T., et al. (2015). Successful arrest of photoreceptor and vision loss expands the therapeutic window of retinal gene therapy to later stages of disease. Proc. Natl. Acad. Sci. USA *112*, E5844–E5853.

52. Komáromy, A.M., Varner, S.E., de Juan, E., Acland, G.M., and Aguirre, G.D. (2006). Application of a new subretinal injection device in the dog. Cell Transplant. *15*, 511–519.

53. Berta, A.I., Boesze-Battaglia, K., Genini, S., Goldstein, O., O'Brien, P.J., Szél, Á., Acland, G.M., Beltran, W.A., and Aguirre, G.D. (2011). Photoreceptor cell death, proliferation and formation of hybrid rod/S-cone photoreceptors in the degenerating STK38L mutant retina. PLoS ONE *6*, e24074.

54. Genini, S., Beltran, W.A., and Aguirre, G.D. (2013). Up-regulation of tumor necrosis factor superfamily genes in early phases of photoreceptor degeneration. PLoS ONE *8*, e85408.

YMTHE, Volume *28*

Supplemental Information

Long-Term Structural Outcomes of Late-Stage *RPE65* Gene Therapy

Kristin L. Gardiner, Artur V. Cideciyan, Malgorzata Swider, Valérie L. Dufour, Alexander Sumaroka, András M. Komáromy, William W. Hauswirth, Simone Iwabe, Samuel G. Jacobson, William A. Beltran, and Gustavo D. Aguirre

Supplemental Fig. 1

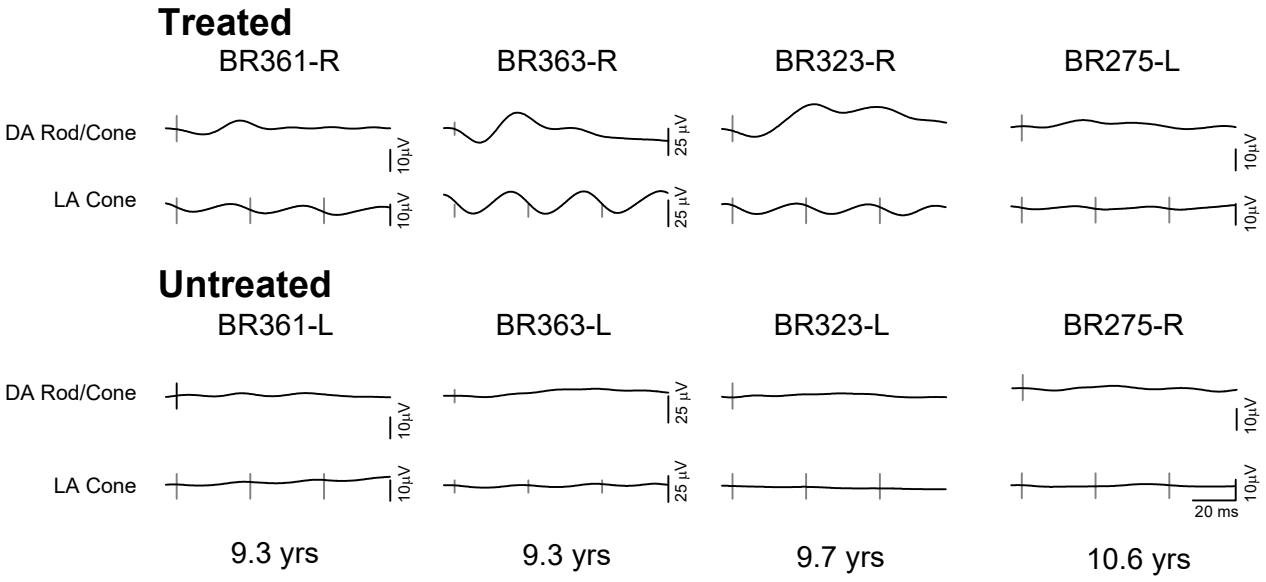

Supplemental Figure 1. Illustration of full-field ERGs recorded from the treated and untreated eyes of RPE65-mutant dogs at the end of study. Shown are the dark-adapted mixed rod-cone responses (DA Rod/Cone) and the light-adapted 29Hz flicker responses (LA Cone). In contrast to untreated eyes, at the end of study all treated eyes had distinct ERG responses under dark- and light-adapted conditions. There was, however, variability in the ERG amplitudes among the treated eyes with BR363-R showing the most robust responses, and BR275-L showing the most reduced responses. There were no recordable responses in untreated eyes.

Supplemental Table 1. Experimental animals and procedures used in the study.

Animal ID	Gender	Status	Tx Age yrs	Vector vol and titer* (dose)	OCT age yrs	Histopathology (PI interval) yrs
BR275	Female	affected		OD: --	6.4, 7.2, 7.5, 7.9, 8.9, 9.4, 10, 10.6 (OS only; cataract OD)	10.6 (4)
			6.6	OS: 190 µL; $3.96x10^{11}$ ($7.5 x10^{10}$ vg)		
BR323	Female	affected	5.3	OD: 200 µL; $3.96x10^{11}$ ($7.9 x10^{10}$ vg)	5.1, 5.6, 6.0, 6.3, 7.3, 7.8, 8.4, 9.1, 9.7 (OU)	9.9 (4.6)
				OS: --		
BR361	Male	affected	4.9	OD: 160 µL; $3.96x10^{11}$ ($6.3 x10^{10}$ vg)	4.8, 5.2, 5.6, 5.9, 6.9, 7.4, 8.0, 8.7, 9.4 (OU)	9.5 (4.6)
				OS: --		
BR363	Female	affected	4.9	OD: 200 µL; $3.96x10^{11}$ ($7.9 x10^{10}$ vg)	4.8, 5.2, 5.5, 5.9, 6.9, 7.4, 8.0, 8.7, 9.4 (OU)	9.5 (4.6)
				OS: --		
BR304	Female	affected	-	--	OU-5.2	5.2
BR318	Female	affected	-	--	OU-5.1, 5.2	5.2
BR354	Female	affected	-	--	OS-5.0	-
CGBCAN, CGBCDI, CGBGS	Male Male Male	WT	-	--	OU-0.7	-
X236 GSK-1 GSK2 D347	Female Male Male Male	WT	-	-	-	8.6 4.3 4.3 6.0

* vector: rAAV2-CMV/CBA-h*RPE65*; vector titer expressed as vector genomes/mL
affected=homozygous for *RPE65* mutation; WT=wildtype control
PI=post-injection; OS= left eye; OD=right eye; OU=both eyes